Jurnal Teknologi, 45(A) Dis. 2006: 81–102

DURABILITY ASSESSMENT OF A NEW FREE PISTON SPARK IGNITION LINEAR ENGINE: A COMPUTATIONAL APPROACH

M. M. RAHMAN[1], A. K. ARIFFIN[2], N. JAMALUDIN[3] & C. H. C. HARON[4]

Abstract. A modern computational approach based on finite element analysis for integrated durability assessment in a two-stroke free piston spark ignition linear engine components is presented. The loading information is difficult to determine without a prototype. The loading histories can be determined using multi-body dynamics. By combining the multi-body dynamics, finite element analysis and fatigue life analysis, the fatigue life of the linear engine components can be predicted early in the design cycle. This paper presents the prediction of fatigue life for free piston linear engine components with complex variable amplitude loadings. The finite element modeling and analysis has been performed using a computer-aided design and finite element analysis software packages, and the fatigue life prediction was carried out using commercial fatigue codes. Crack initiation approach is applied to predict the fatigue life of the component of a free piston linear engine. The results are expected to show contour plots of fatigue life, and damage histogram at the worst or most damaging case. The obtained results indicate that when using the loading sequences is predominantly tensile in nature (SAETRN loading), the SWT and the Morrow models give shorter life than that results obtained using the Coffin-Manson model. However, the Coffin-Manson method gives conservative prediction when the time histories are predominantly compressive, and zero mean stress loadings. It was also observed that the damage to be generated from the cycles is in the higher stress range.

Key words: Durability, fatigue life, finite element, multi-body dynamics, free piston linear engine.

Abstrak. Pendekatan pengkomputeran moden yang berasaskan analisis unsur terhingga untuk penilaian ketahanan dalam komponen enjin linear palam pencucuh piston bebas dua lejang dibentangkan. Maklumat pembebanan adalah sukar ditentukan tanpa sebarang prototaip. Sejarah pembebanan boleh ditentukan menggunakan dinamik multi-jasad. Dengan menggabungkan dinamik multi-jasad, analisis unsur terhingga dan analisis hayat lesu, hayat lesu bagi enjin linear boleh diramal awal semasa reka bentuk. Kertas kerja ini membentangkan ramalan hayat lesu bagi komponen enjin linear piston bebas dengan pembebanan amplitud berubah. Permodelan dan analisis unsur terhingga dijalankan menggunakan reka bentuk terbantu komputer dan perisian analisis unsur terhingga serta ramalan hayat lesu adalah menggunakan kod lesu komersial. Pendekatan permulaan retak digunakan bagi meramal

[1-4] Computational and Experimental Mechanics Group, Department of Mechanical and Materials Engineering, Universiti Kebangsaan Malaysia 43600 UKM, Bangi, Selangor DE, Malaysia.
[1] Corresspondense Phone:+6(03)89216012; Fax: +6(03)89216040, e-mail: mustafiz@eng.ukm.my

hayat lesu komponen bagi enjin linear piston bebas. Keputusan yang diharapkan adalah plot kontur hayat lesu dan histogram kerosakan pada kes yang paling rosak. Keputusan yang diperolehi menunjukkan bila menggunakan rangkaian beban tegangan yang lebih banyak (beban SAETRN), SWT dan Morrow memberikan hayat lebih singkat daripada model Coffin Manson Walau bagaimanapun, kaedah Coffin-Manson memberikan ramalan yang konservertif bila sejarah masa beban mampatan lebih banyak dan tegasan min sifar. Keputusan juga menunjukkan julat tegasan yang besar juga menyumbang lebih besar kerosakan.

Kata kunci: ketahanan, hayat lesu, unsur terhingga, dinamik multi-jasad, enjin linear piston bebas.

1.0 INTRODUCTION

A two-stroke free piston spark ignition linear generator (LG) engine integrates with a combustion engine and a linear electrical machine into a single unit without a crankshaft. This provides an unconventional solution for series hybrid vehicles and distributes/emergency power units [1-7]. The free piston engine consists of a double-ended piston, double-ended cylinder, and a linear alternator. The piston is enclosed inside a double-ended cylinder where it moves freely along the cylinder's axis. Combustion of a premixed fuel-air charge occurs successively at opposite ends of the cylinder creating the driving force for piston oscillation. Rare earth magnets are fixed on the piston so that their oscillating motion creates a varying magnetic flux within the alternator core. The alternator converts this changing flux into electricity, directly harnessing the mechanical work of the piston as electrical power. The dynamics of the piston are moderated by the linear alternator which controls the electromagnetic force on the piston. The alternator precisely manages the piston's kinetic energy so that the desired compression ratio is reached on each piston stroke [8].

The piston engine is unique in that there is no crankshaft, or any of the mechanical linkages typically found in reciprocating IC engines; Due to this unique arrangement, the piston oscillates freely within the cylinder. The achievable compression ratio is thus only a function of the piston's inertia, not dependent on the structure or rigidity of any mechanical linkages. The compression ratio in this engine is variable, and potentially much greater than in the conventional configurations. Bulky designs are not necessary criteria to achieve substantial compression ratios in the free piston configuration [9,10]. The schematic diagram of a two-stroke free piston linear generator engine is shown in Figure. 1

The useable compression ratio of the free piston engine is however dependent on the characteristics of the fuel on which the engine operates. The premixed fuel-air charge must be able to withstand the inclination to autoignite through the compression stroke; and once at top-dead-centre (TDC) the mixture must initiate and burn completely before the piston reverses its direction [8]. Due to its

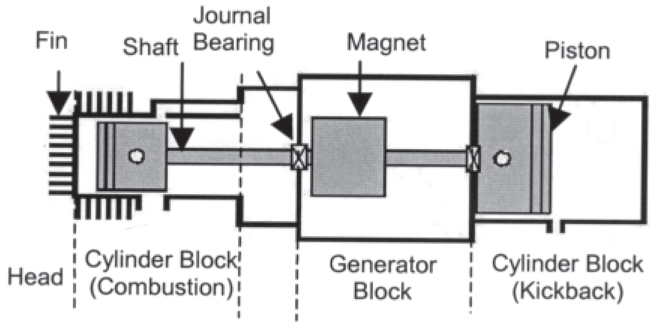

Figure 1 A two-stroke free piston linear generator engine

unique characteristics, hydrogen represents an ideal fuel for this application: operating at sufficiently low equivalence ratios, the compression ratio required to induce autoignition is increased [11]. However, hydrogen's low ignition energy ensures that the induction time, and thus burning duration is relatively short [12, 13]. Equivalence ratio is defined as the ratio of the actual fuel to the stoichiometric ratio. As a result, the free piston engine operating on hydrogen is expected to achieve operating compression ratios in the range of 20-30:1 a completely unrealistic expectation for conventionally fueled SI engine [8, 14, 15].

Most of the previous studies [1-7, 16-19] related to the LG engine utilizes two combustion chamber in order to get the linear movement of the piston. For this linear engine, crank and camshaft will not be required and there was no rotary movement involved. In addition, the linear system of the engine should prove to be more efficient as the frictional losses associated with the crack and rod bearings are not present. However, the previous study [19] used a single piston engine with rebound device and the system tended to create unbalanced situation. These need to be encounter for in this new free piston generator engine design.

Durability is one of the most important design requirements that are essential for a new engine product to achieve successful market competitiveness. For the vehicle body structure the durability assessment has traditionally been performed at the later part of the product development stage when prototypes are available, and heavily relied upon the result of the ground durability tests. This process is very time consuming and often results in over-design with weight penalties, which is the major obstacle to achieve fuel economy. Due to the development in the computer-aided engineering (CAE) tools, a three-step process that includes multibody dynamic analysis, finite element analysis, and fatigue life prediction, is widely used today for early product durability evaluation [20-23]. This approach helps the designer to acquire the necessary information for continuous design analysis, and predicts the durability of the free piston linear generator engine in the early design stage, thereby eliminating some of the shortcomings in the traditional durability evaluation method.

For the durability analysis of the linear generator (LG) engine components in a multi-body dynamic system, substantial improvements have been made to efficiently obtain dynamic stress histories using dynamic simulation methods [24-26], and fatigue life using stress-based or strain-based methods [27-31]. Ryu *et al.*, [26] developed an efficient method that combines the flexible multibody dynamic simulation and quasi-static finite element analysis to compute the dynamic stress histories. The local strain-based fatigue life prediction methods are used widely because they are easy to implement, provide a reasonable "first approximation" for a multiaxial fatigue crack initiation, and utilize a large amount of available uniaxial fatigue data. In this research von Mises equivalent strain method is used to predict the fatigue life of two-stroke free piston engine components.

However, the durability of two-stroke free piston engine has rarely been studied because it is a multidisciplinary research problem that involves multibody dynamics, structural analysis, and fatigue life prediction. Moreover, due to the requirement of the peak-valley editing and rainflow counting procedure in the fatigue life prediction, an analytical relationship between the dynamic stress and the fatigue life can not be obtained easily. Thus it becomes extremely difficult, if not impossible, to obtain the fatigue life design analytically. The objectives of this paper are to predict the fatigue life of a free piston linear engine cylinder block using nominal stress-life, normal strain-life fatigue prediction methods and also to investigate the effect of mean stress on the fatigue life.

2.0 PROPOSED DURABILITY ANALYSIS

Durability analysis can be used to determine how long a component can survive in a given service environment. In a general case, durability refers to the ability of a component to function in the presence of defects for a given environment/ loading. In practice, however, the predominant failure mode is fatigue and hence, the term durability analysis will be used to describe the analysis of a fatigue performance.

Fatigue of materials is a very complex process, and has not been fully understood up to now. The majority of the components designs involve parts subjected to fluctuating or cyclic loads. Fatigue analysis has traditionally been performed at a later stage of the design cycle. This is due to the fact that the loading information could only be derived from direct measurements, which require a prototype [29-31]. Multibody dynamics (MBD) [32] is capable of predicting the component loads which enable design engineer to undertake a durability assessment even before a prototype is fabricated. The purpose of analysing a structure early in the design cycle is to reduce the development time and cost. This is achieved by determining the critical regions of a structure and improving the design before prototypes are built and tested. Three computational processes are utilized to perform the durability analysis using CAE tools. The processes are as follows:

(i) Multibody dynamic simulation- to determine the loading on a component based on system inputs;
(ii) Finite Element Analysis (FEA)- to determine the stress/strain state of a component for a given load condition;
(iii) Fatigue Analysis- to calculate the fatigue life for the component of interest and identify the critical locations.

Fatigue analysis is used to compute the fatigue life at single location in a structure. For multiple locations the process is repeated using geometry information applicable for each location. The required inputs for the fatigue analysis process are shown in Figure 2. The three input information are descriptions of the material properties, loading histories and geometry. The details of these inputs are as follows:

(i) Material information - cyclic or repeated material data based on a constant amplitude testing.
(ii) Load histories information - measured or simulated load histories applied to a component. The term “loads” is used to represent forces, displacements, accelerations, etc.
(iii) Geometry information - relates the applied load histories to the local stresses and strains at the location of interest. The local stresses and strains information are usually derived from the finite element (FE) results.

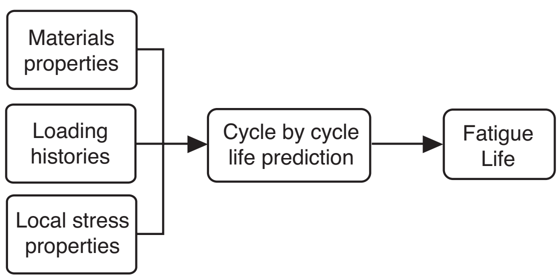

Figure 2 Schematic diagram of fatigue life estimation

The finite element analysis results define the stress-state for a component given the specific loading condition. The most common FE analysis method used in conjunction with fatigue analysis is to apply each load independently as a unit load case. The inputs for the FE analysis are the component geometry with FE model, the boundary conditions, and the loading information. The location and direction of each load input define the loading information. The finite element method assumes that component behavior and material properties are linearly elastic. The linear static superposition is used to combine the loading histories and the FE analysis results to calculate the local pseudo-stress history for an element. The local pseudo-stress history is corrected to take into account for any elastic-plastic behavior. Fatigue analysis is performed for that element, and the process is then repeated for each element (or node) within the FE model. The general process of finite element based fatigue analysis is shown in Figure 3.

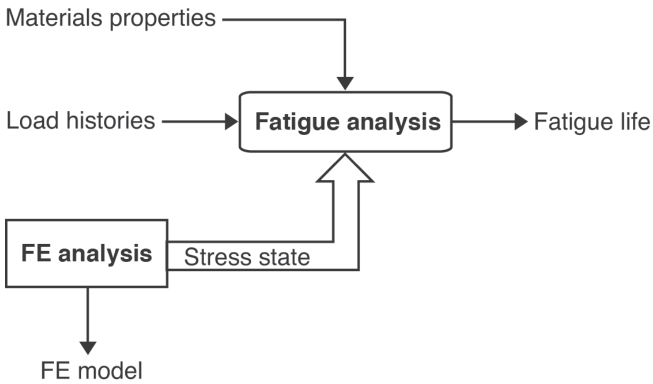

Figure 3 The finite element based fatigue analysis

The FE based durability analysis can be considered as a complete engineering analysis for the components. The fatigue life can be estimated for every element in the finite element model, and the contour plots of life or damage. Geometry information is provided by the FE results for each load case applied independently. Appropriate material properties are also provided for the desired fatigue analysis method. An integrated approach to durability analysis combines the multibody dynamic analysis, finite element analysis, and the fatigue analysis into a consistent entity for the prediction of the durability of a component. The process of finite element based integrated durability analysis is shown in Figure 4.

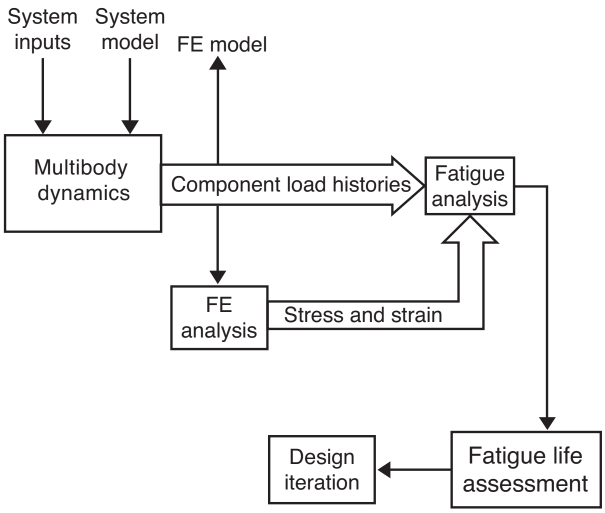

Figure 4 The proposed finite element based integrated durability analysis

3.0 FATIGUE ANALYSIS METHODS

Fatigue analyses can be undertaken by using either one of the three basic methodologies including the stress-life approach, crack initiation (strain-life) approach, and crack propagation (crack growth) approach. The stress-life method was first applied over a hundred years ago [33] and considers nominal elastic stresses and how they are related to life. Life is usually defined as catastrophic failure. The initiation or strain-life approach, which evolved some fifty years ago, considers elastic-plastic stresses and strains. It represents a more fundamental approach and is used to determine the number of cycles required to initiate a small engineering cracks. Crack propagation or linear elastic fracture mechanics (LEFM) approach is used to predict how quickly pre-existing cracks grow and also to estimate how many loading cycles are required to cause the cracks to reach a critical size when catastrophic failure would occur.

An important aspect of the fatigue process is the plastic deformation. Fatigue cracks initiate from the plastic straining in the localized regions. Therefore, the cyclic strain-controlled fatigue method can better characterize the fatigue behaviour of the materials compared to the cyclic stress-controlled fatigue. This is particularly true in the notched members, where significant localized plastic deformation is often present. In crack initiation approach the plastic strain or deformation is directly measured and quantified. The stress-life approach does not take into account the plastic strain. One of the main advantages of the crack initiation approach is that it accounts for changes in local mean and residual stresses. Due to the fact that the load history contains large overloads and significant plastic deformation; the crack initiation approach is generally superior to the stress-life approach for fatigue life prediction. However, for a relatively low level load in which the resulting strains are mainly elastic, the crack initiation and stress-life approaches usually yield similar prediction results. At present, the crack initiation approach to fatigue problems is widely used, especially during the starting or stopping process of the free piston engine in which it is subjected to a very high stress range. Due to the above reasons, the crack initiation method is considered and briefly discussed in this paper.

The crack initiation (FCI) approach involves the techniques for converting the loading history, geometry, and materials properties (monotonic and cyclic) input into a fatigue life prediction. The operations involved in the prediction process must be performed sequentially. First, the stress and strain at the critical region are estimated, and the rainflow cycle counting method [34] is then used to reduce the load-time history based on the peak-valley sequential. The next step is to use the finite element method to convert the reduced load-time history into a strain-time history and also to calculate the stress and strain in the highly stressed area. Then, the crack initiation methods are employed to predict the fatigue life. The simple linear hypothesis proposed by Palmgren [35] and Miner [36] is used to accumulate fatigue damage. Finally, the damage values for all cycles are summed until a critical damage sum (failure criteria) is reached.

In order to perform fatigue analysis and to implement the stress-strain approach in complex structures, Conle and Chu [37] used the strain-life result which is simulated using three-dimensional models to assess the fatigue damage. After the complex load history was reduced to an elastic stress history for each critical element, a neuber plasticity correction method was used to correct the plastic behaviour. Elastic unit load analysis using strength of materials and an elastic finite element analysis model combined with a superposition procedure of each load point's service history was proposed. Savaidis [38] verified that the local strain approach is suitable for a durability evaluation. In this study, it was observed that the local strain approach using the Smith-Watson-Toper (SWT) strain-life model is able to represent and to estimate many parameters explicitly. These include mean stress effects, load sequence effects above and below the endurance limit, and manufacturing process effects such as surface roughness and residual stresses, and also stated by Juvinall and Marshek [39].

The fatigue resistance of metals can be characterized by a strain-life curve. These curves are derived from the polished laboratory specimens tested under completely reversed strain control. The relationship between the total strain amplitude, $\Delta\varepsilon/2$, and the reversals to failure, $2N_f$, can be expressed in the following form [40-41]. The Coffin-Manson total strain-life is mathematically defined as Equation (4).

$$\frac{\Delta\varepsilon}{2} = \frac{\sigma'_f}{E}(2N_f)^b + \varepsilon'_f\,(2N_f)^c \tag{4}$$

where N_f is the fatigue life; σ'_f is the fatigue strength coefficient; E is the modulus of elasticity; b is the fatigue strength exponent; ε'_f is the fatigue ductility coefficient; and c is the fatigue ductility exponent. The typical strain-life curves based on Coffin-Manson relationship are shown in Figure 5

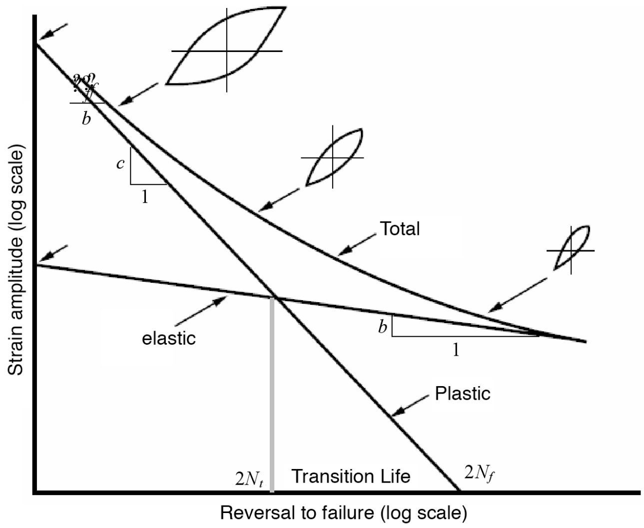

Figure 5 A typical strain-life curve

Morrow [42] suggested that the mean stress effects could be considered by modifying the elastic term in the strain-life equation by mean stress, σ_m.

$$\varepsilon_a = \frac{\sigma'_f - \sigma_m}{E}(2N_f)^b + \varepsilon'_f(2N_f)^c \tag{5}$$

Smith *et al.*, [43] introduced another mean stress model which is called Smith-Watson-Topper (SWT) mean stress correction. It is mathematically defined as:

$$\sigma_{\max}\varepsilon_a E = \left(\sigma'_f\right)^2(2N_f)^{2b} + \sigma'_f\,\varepsilon'_f\,E\,(2N_f)^{b+c} \tag{6}$$

where, $\sigma_{\max}$ is the maximum stress, and ε_a is the strain amplitude.

4.0 MATERIAL INFORMATION

The material properties is one of the major input, which is the definition of how a material behaves under cyclic loading conditions typically experienced by materials during service operation. Cyclic material properties are used to calculate the elastic-plastic stress strain response and the rate at which fatigue damage accumulates due to each fatigue cycle. The materials parameters required depend on the analysis methodology being used. Normally, these parameters are measured experimentally and are available in various handbooks. Two different materials were used for the cylinder block of the free piston engine, AA5083-87-CF and AA6061-T6-80-HF. Their characteristics are discussed in the following sections. The mechanical properties of the two aluminum alloys are tabulated in Table 1.

Table 1 Summary of the mechanical properties of the two aluminum alloys [44]

Properties	**Aluminum Alloy**	
	AA5083-87-CF	**AA6061-T6-80-HF**
Monotonic Properties		
Modulus of elasticity, E (GPa)	69.0	72.7
Yield Strength, YS (MPa)	285	313
Ultimate strength, S_u (MPa)	385	340
Strength Coefficient, K (MPa)	466	402
Strain hardening exponent, n	0.081	0.043
Fracture toughness, K1C(MPa-m$^{1/2}$)	43	29
Cyclic and fatigue Properties		
Fatigue strength coefficient, σ'_f (MPa)	650	645
Cyclic strength coefficient, K' (MPa)	417	416
Cyclic strain hardening exponent, n'	0.035	0.042
Fatigue strength exponent, b	– 0.094	– 0.097
Fatigue ductility coefficient, ε'_f	2.26	0.22
Fatigue ductility exponent, c	–1.01	– 0.6
Fatigue limit, S_f@2×10^8 cycles (MPa)	133.85	126.29

Figures 6 and 7 show the monotonic and cyclic stress-strain curves of these two materials, respectively. The figures show how these two materials behave under cyclic loading conditions and how they behave relative to one another. For the cyclic loading, it can be seen that the aluminum alloy AA5083-87-CF has higher strength with its yield point well above that of the AA6061-T6-80-HF. However, for the monotonic loading conditions, the AA6061-T6-80-HF is found to have higher strength compared with the AA5083-87-CF.

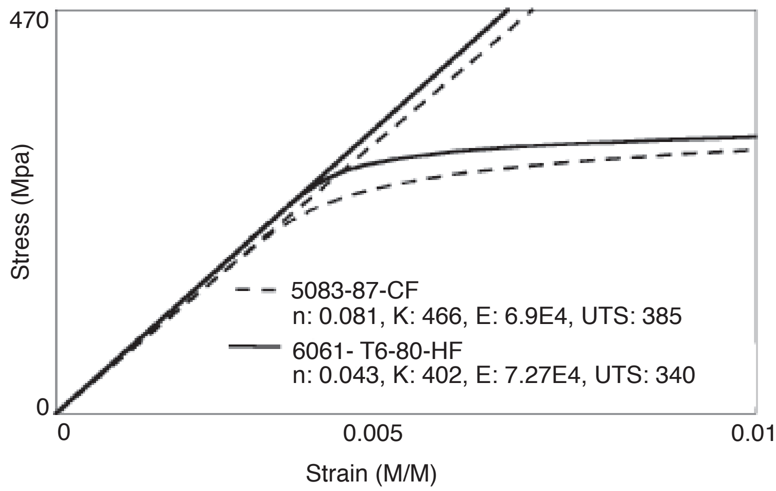

Figure 6 Monotonic stress-strain curves of 5083-87-CF and 6061-T6-80-HF

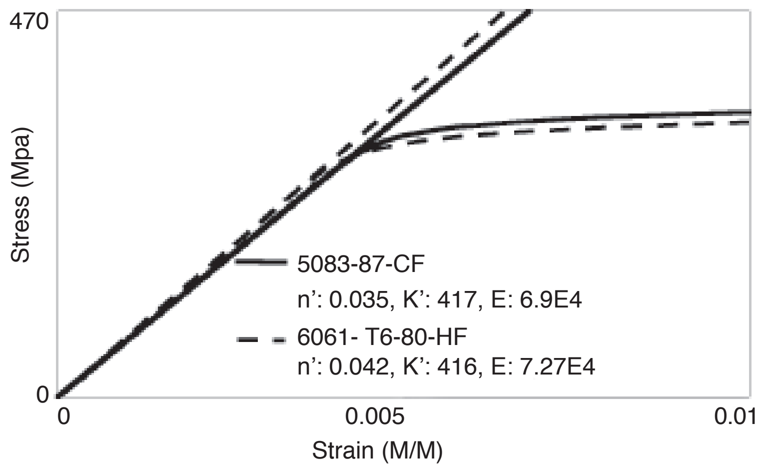

Figure 7 Cyclic Stress-strain curves of 5083-87-CF and 6061-T6-80-HF

Figures 8 and 9 represent the cyclic and monotonic stress-strain curves for the AA5083-87-CF and the AA6061-T6-80-HF, respectively. It can be seen that both the materials cyclic yield strength is higher that that of monotonic yield strength. This implies that both the materials are stronger under cyclic loading *i.e.*, cyclic hardening or strain hardening.

Figure 10 represents the strain-life curves for both materials. The figure clearly shows that the materials have different fatigue life behaviour. Figure 11 is plotted based on the SWT relationship. From the figure, it can be seen that the differences in the figure life behaviour is significant in the short life (low cycle

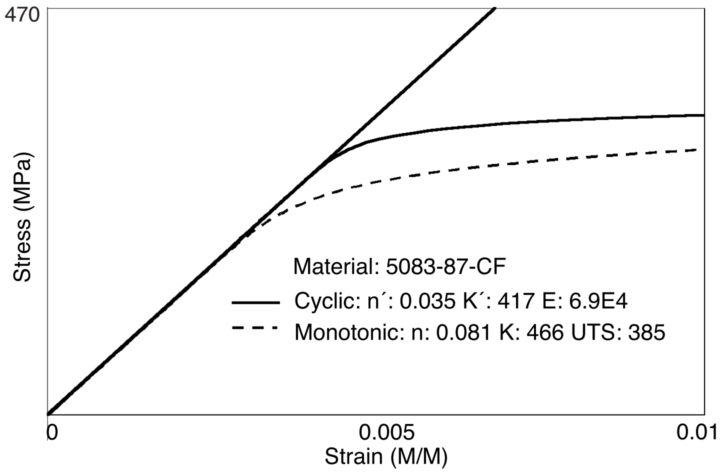

Figure 8 Cyclic and monotonic stress-strain curves of AA5083-87-CF

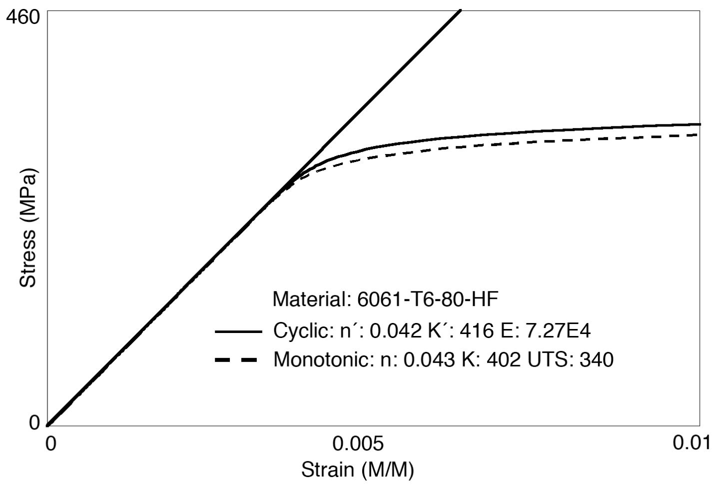

Figure 9 Cyclic and monotonic stress-strain curves of 6061-T6-80-HF

fatigue). On the other hand, the differences becomes less significant in the long life are (high cycle fatigue).

5.0 LOADING INFORMATION

Loading is another major input to the finite element based fatigue analysis. Several types of variable amplitude loading history were selected from the Society of Automotive Engineers (SAE) profiles. The component was loaded with three random time histories, corresponding to typical histories for transmission, suspension and bracket components at different load levels. The

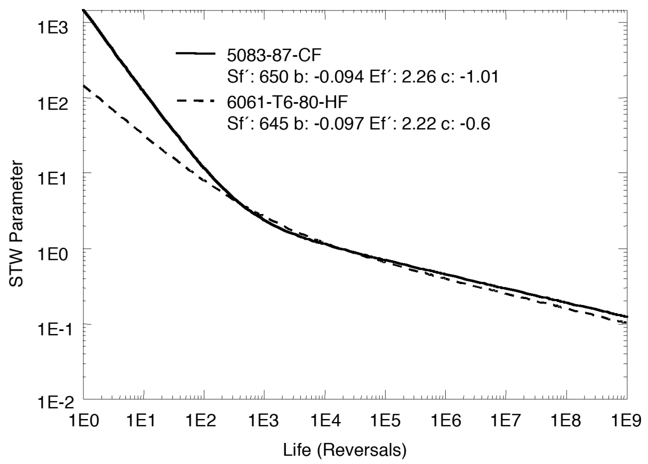

Figure 10 Smith-Watson-Topper life curves of 5083-87-CF and 6061-T6-80-HF

detailed information about these histories can be referred in the literature [45]. These histories were scaled to two peak strain levels and used as full-length histories. In addition, a random history including many spikes was selected for the simulation of spike removal. The variable amplitude load-time histories are shown in Figure 11. The terms of SAETRN, SAESUS, and SAEBRAKT represent the load-time history for the transmission, suspension, and bracket respectively. The considered load-time histories are based on the SAE's profile. The abscissa is the time, in seconds.

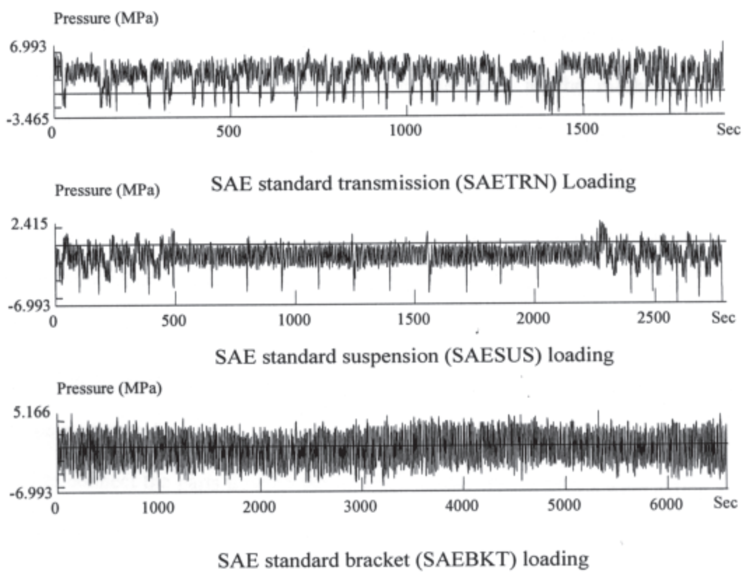

Figure 11 The variable amplitude load-time histories

6.0 NUMERICAL EXAMPLE

A geometric model of the cylinder block of the free piston engine is considered in this study. There are several contact areas including cylinder head, gasket, and hole for bolt. Therefore, constraints are employed for the following purposes: (i) to specify the prescribed enforce displacements, (ii) to simulate the continuous behavior of displacement in the interface area, (iii) to enforce rest condition in the specified directions at grid points of reaction. Three-dimensional model of free piston linear engine cylinder block was developed using CATIA® software. A parabolic tetrahedral element was used for the solid mesh. Sensitivity analysis was performed to obtain the optimum element size. These analyses were performed iteratively at different element lengths until the solution obtained with appropriate accuracy. Convergence of the stresses was observed, as the mesh size was successively refined. The element size of 0.20 mm was finally considered. A total of 35415 elements and 66209 nodes were generated with 0.20 mm element length. Compressive loads were applied as pressure (7 MPa) acting on the surface of combustion chamber and preloads were applied as pressure (0.3 MPa) acting on the bolt-hole surfaces. In addition preload was also applied on the gasket surface generating pressure of 0.3 MPa. The Multi-point Constraints (MPCs) were applied on the bolt-hole for all six degree of freedom. Multi-point constraints [46] were used to connect the parts through the interface nodes. These MPCs were acting as an artificial bolt and nut that connect each parts of the structure. Each MPC's will be connected using a Rigid Body Element (RBE) that indicates the independent and dependent nodes. The configuration of the engine is constrained by bolting the cylinder head and the cylinder block. In the condition with no loading configuration, the RBE element with six-degrees of freedom were assigned to the bolts and the hole on the cylinder head. The independent node was created on the cylinder block hole. Due to the complexity of the geometry and loading on the cylinder block, a three-dimensional FEM was adopted as shown in Figure12. The loading and constraints on the cylinder block are shown in Figure13.

The linear static finite element analysis was performed using MSC.NASTRAN® finite element software. The bolt - holes areas were found to experience the highest stresses. The maximum principal stresses and strains are used for the subsequent fatigue life analysis and comparisons. The maximum principal stresses distribution of cylinder block for the linear static analysis is presented in Figure 14. From the acquired results, the maximum principal stress of 23.4 MPa occurring at node 92190 was obtained. The fatigue life of the cylinder block is predicted using variable amplitude loading conditions (see Figure 11). The predicted fatigue life results of the cylinder block corresponding to 99.6% reliability value are shown in Figure 15. From the results, it is shown that the predicted fatigue life of the AA6061-T6-80-HF aluminum alloy at the most critical location, near the bolt-hole edge (node 92190), is $10^{3.44}$ seconds using the Coffin-Manson method. The fatigue life is represented in terms of seconds using the variable amplitude SAESUS loading histories. The fatigue equivalent unit is 3000 cpm (cycle per min) of the time history. The critical locations are shown in Figure 15 using the SAESUS loading histories. It is found that the bolt-hole edge is the most critical positions for the cylinder block.

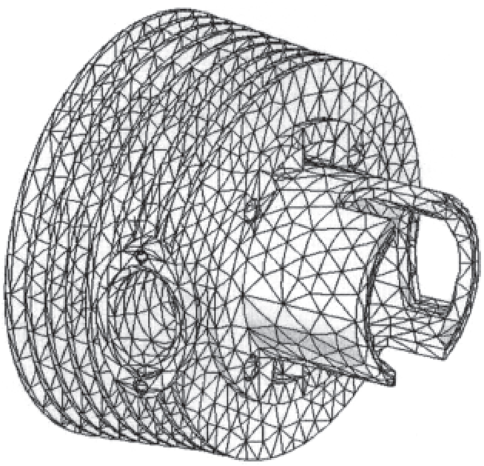

Figure 12 Three-dimensional finite element model

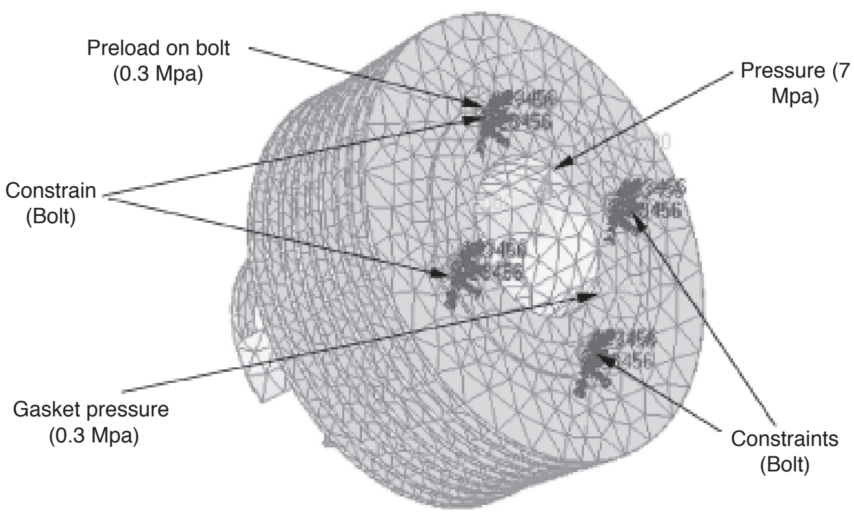

Figure 13 The loading, boundary conditions and constraints

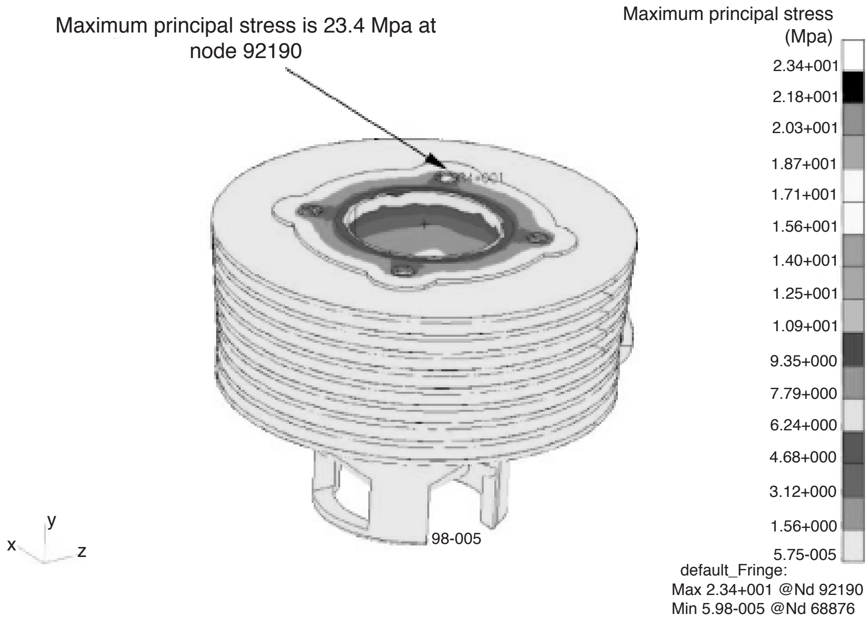

Figure 14 The maximum principal stresses distribution

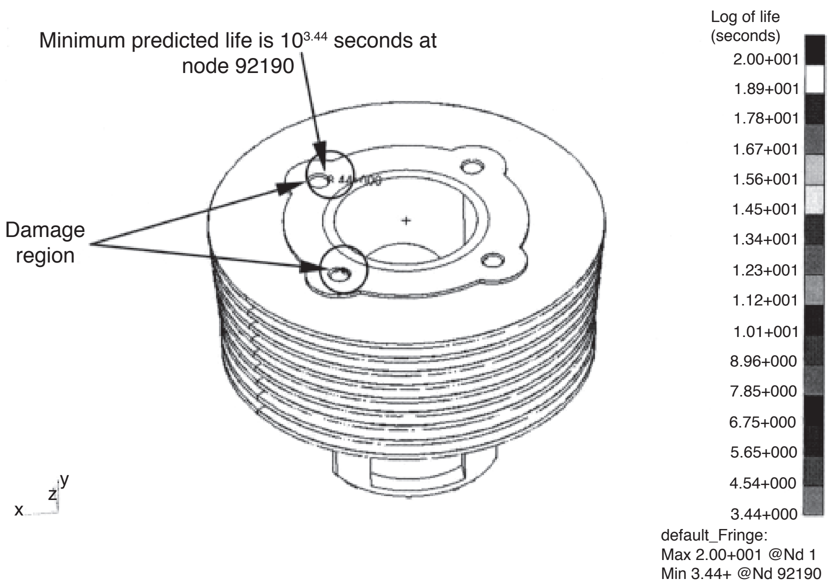

Figure 15 Predicted Fatigue log of life contour for SAESUS loading conditions

Most realistic service situations involve nonzero mean stresses. It is, therefore, vital to know the influence of the mean stress on the fatigue process with the fully reversed (zero mean stress) laboratory data normally employed in the assessment of real situations. Two mean stress correction methods are considered in this study including the SWT and the Morrow mean stress correction methods. It is difficult to categorically select one procedure in preference to the other. The predicted fatigue life at most critical location using different loading histories are tabulated in Table 2. It is observed that when using the loading sequences which predominantly tensile in nature (SAETRN loading), the SWT, and the Morrow methods give shorter life than that results obtained by the Coffin-Manson model. However, for the predominantly compressive loading (SAESUS), particularly for wholly compressive cycles, the SWT, and the Morrow's methods are found to give longer life than the Coffin-Manson model. When using the time history roughly zero mean loading (SAEBRAKT), all the three methods give approximately similar results. Table 3 summarises the results of the fatigue life predicted using the SAESUS loading conditions for the different aluminum alloys. From Table 3, it is also observed that the predominantly tensile (positive) mean loading produces longer life than the compressive mean loading (SAESUS). It shows that the AA7175-T73 alloy is the most superior material having the longest life among the aluminum alloys while the AA4032-T6 is found to be the weakest material. In designing for durability, the presence of a nonzero mean stress can influence the fatigue behaviour of materials because a tensile or a compressive mean stress has been shown to be responsible for accelerating or decelerating crack initiation. It is observed that the compressive mean stresses are beneficial while the tensile mean stresses are detrimental to the fatigue life. This phenomenon is dominant when the mean stress levels are relatively low compared with the cyclic yield stress and the fatigue behaviour falls in the long-life regime where elastic strain is dominant.

Table 2 Predicted fatigue life at most damage location (node 92190)

Loading conditions	**Predicted fatigue life in hours**					
	AA5083-87-CF			**AA6061-T6-80-HF**		
	SWT	Morrow	Coffin-Manson	SWT	Morrow	Coffin-Manson
SAETRN	9.73×10^4	2.31×10^5	4.80×10^5	2.87×10^5	7.05×10^5	1.57×10^6
SAESUS	6.36×10^3	7.36×10^3	5.47×10^3	1.68×10^4	1.17×10^4	5.62×10^3
SAEBRAKT	3.60×10^3	3.38×10^3	2.98×10^3	1.02×10^4	9.48×10^3	8.97×10^3

Table 3 Predicted fatigue life for different aluminum alloys at most damage location using the SAESUS loading histories

Materials (Aluminum alloys)	Predicted life in hours SWT	Morrow	Coffin-Manson
AA2014-T6	1.53×10^5	2.59×10^4	1.01×10^4
AA2024-T6	2.28×10^4	1.03×10^4	4.61×10^3
AA2024-T86	4.27×10^5	8.34×10^4	2.55×10^4
AA2048	9.62×10^4	3.02×10^4	1.09×10^4
AA2090-T86	5.72×10^5	1.01×10^5	3.01×10^4
AA4032-T6	2.19×10^3	1.46×10^3	949
AA5083-87	1.68×10^4	1.17×10^4	5.62×10^3
AA5454	5.44×10^3	6.37×10^3	5.04×10^3
AA6009-T9	5.42×10^3	3.52×10^3	2.22×10^3
AA6053-T6	2.90×10^4	1.44×10^4	6.95×10^3
AA6061-T6	1.68×10^4	1.17×10^4	5.62×10^3
AA6069-T6	7.09×10^4	2.42×10^4	9.13×10^3
AA6151-T6	4.05×10^3	2.73×10^3	`1.80×10^3
AA6262-T9	3.67×10^4	1.74×10^4	8.06×10^3
AA6061-T6	6.36×10^3	7.36×10^3	5.47×10^3
AA7075-T6	3.24×10^6	2.95×10^5	7.88×10^4
AA7175-T73	4.80×10^6	5.87×10^5	8.71×10^4

The Three-dimensional cycle histogram and the corresponding damage histogram for the AA6061-T6-80-HF aluminum alloy using SAESUS loading histories are shown in Figures 16 and 17, respectively. Figure 16 shows the results of the rainflow cycle count for the critical location on the component. It is observed that there are a lot of cycles at the low stress range. However, the cycles significantly decrease at the high stress range. The height of each tower represents the number of cycles at that particular stress range and mean. Figure 17 indicates that the lower stress ranges produced zero damage. The figure also shows that most of the damages are found to occur at the high stress ranges. The damages at the higher ranges are found to be widely distributed which means that it cannot point to a single event causing damage.

Local single location fatigue analysis usually comes in the forms of a histogram of rainflow range cycles or damage [47]. Joint plot of cycle histogram and corresponding damage histogram for the AA6161-T6 using the SAESUS loading histories is shown in Figure 18. The figure shows both the results of the rainflow cycle count and the damage for the critical location on the component. It is also observed that the lower stress ranges produced zero damage. All the damage is observed to be generated from the cycles in the higher stress range, which would be expected.

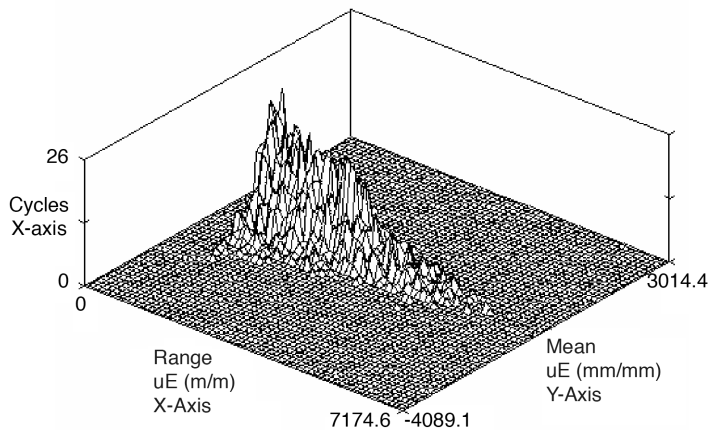

Figure 16 The cycle histogram of critical location for AA6061-T6-80-HF

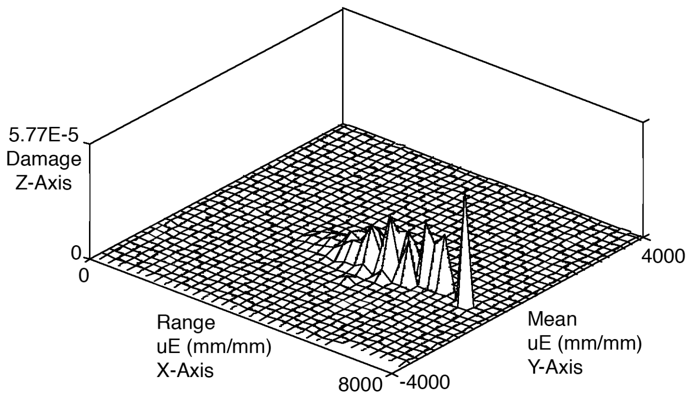

Figure 17 The damage histogram of critical location for AA6061-T6-80-HF

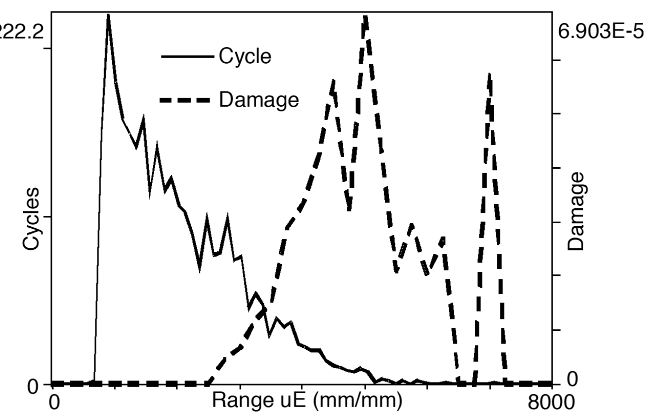

Figure 18 Combined plot of histogram of damage and rainflow range cycles

7.0 CONCLUSION

A computational approach of the fatigue analysis methodology for the life prediction is presented. Based on the conducted study, several conclusions can be drawn with regard to the fatigue life prediction of a two-stroke free piston engine when subjected to complex variable amplitude loading conditions. The obtained results indicate that the influences of mean stress correction are different for the compressive and the tensile mean stress. The predicted fatigue life appears to be more conservative for the tensile mean stress than the compressive mean stress. In designing for durability, the presence of a nonzero mean stress can influence fatigue behaviour of materials because a tensile or a compressive mean stress has been shown to be responsible for accelerating or decelerating the crack initiation process. It is concluded that the compressive mean stresses are found to be beneficial and tensile mean stresses are detrimental to the fatigue life. It can also be concluded that the higher stress ranges produce more damage. Therefore the proposed approach can be used an efficient and reliable means for the durability assessment of a prototype engine with actual service environments in the early-developing stage.

ACKNOWLEDGMENTS

The authors would like to thank the Department of Mechanical and Materials Engineering, Universiti Kebangsaan Malaysia. The authors are also grateful to the Ministry of Science, Technology and Innovation, Malaysia under IRPA project (No: 03-02-02-0056 PR0025/04-03) for providing financial support.

REFERENCES

[1] Zhang, X., J. Katzberg, B. Cooke, and J. Kos. 1997. Modeling and Simulation of a Hybrid Engine. *Proceedings of the IEEE WESCANEX 97: Communications, Power and Computing.* Manitoba, Canada. 286-291.

[2] Blarigan, P. V. 2000. Advanced Internal Combustion Engine Research. *Proceedings of the 2000 DOE Hydrogen Program Review:* NREL/CP-570-28890. CA, USA. 1-19.

[3] Goertz, M., and L. Peng. 2000. Free Piston Engine and its Application and Optimization. *SAE Technical Paper Series*, Paper no. 2000-01-0996. 1-10.

[4] Arshad, W. M., C. Sadarangani, T. Bäckström, and P. Thelin. 2002. Finding an Appropriate Electrical Machine for a Free Piston Engine Generator. *Proceedings of the 19th International Battery, Hybrid and Fuelcell Electrical Vehicle Symposium (EVS-19).* Busan, Korea. 427-438.

[5] Arshad, W. M., P. Thelin, T. Bäckström, and C. Sadarangani. 2003. Alternative Electrical Machine Solutions for a Free Piston Generator. *Proceedings of the 6th International Power Engineering Conference.* Singapore. 329-334.

[6] Cosic A., J. Lindbäck, W. M. Arshad, M. Leksell, P. Thelin, and E. Nordlund. 2003. Application of a Free Piston Generator in a Series Hybrid Vehicles. *Proceedings of the 4th International Symposium on Linear Drives for Industrial Applications* (LDIA 2003). Birmingham, England. 541-544.

[7] Arshad, W. M., P. Thelin, T. Bäckström, and C. Sadarangani. 2004. Use of Transverse Flux Machines in a Free Piston Generator. *IEEE Transactions on Industry Applications.* 40(4): 1092-1100.

[8] Van Blarigan, P. 1998. Advanced Hydrogen Fueled Internal Combustion Engines. *Energy and Fuels.* 12: 72-77.
[9] Achen, P. A. J. 1994. A Review of Free Piston Engine Concepts. *SAE Technical Paper* 941776.
[10] Somhorst, J. H. E., and P. A. J. Achten. 1996. The Combustion Process in a DI Diesel Hydraulic Free Piston Engine. *SAE Technical Paper,* Paper No 960032.
[11] Homan, H. S., R. K. Reynolds, P. C. T. de Boer, and W. J. Mclean. 1979. Hydrogen Fueled Diesel Engine without Timed Ignition. *International Journal of Hydrogen Energy.* 4: 315-325.
[12] King, R. O., and M. Rand. 1955. The Oxidation, Decomposition, Ignition, and Detonation of Fuel Vapors and Gases, XXVII, The Hydrogen Engine. *Canadian Journal of Technology.* 33: 445-469.
[13] Gathercole, A. H., J. P. Bindon, and L. W. Roberts. 1980. Detonation Limited Air Fuel Ratios in a Conventional High Speed Spark Ignition Engine Fueled with Hydrogen. *The South African Mechanical Engineer.* 30: 257-263.
[14] Bolt, J. A., and D. H. Holkeboer. 1962. Lean fuel/air Mixtures for High Compression Spark-ignited Engines. *SAE Transactions.* 70: 195-202.
[15] Caris, D.F., and E. E. Nelson. 1959. A New Look at High Compression Engines. *SAE Transactions.* 67: 112-124.
[16] Famouri, P., W. R. Cawthrne, N. Clark, S. Nandhumar, C. Atkinson, R. Atkinson, T. McDaniel, and S. Petreanu. 1999. Design and Testing of a Novel Linear Alternator and Engine System for Remote Electrical Power Generator. *Proceedings of the IEEE Power Engineering Society Winter Meeting 1999.* New York, USA. 108-112.
[17] Arshad, W. M., T. Bäckström, P. Thelin, and C. Sadarangani. 2002. Integrated Free Piston Generators: An Overview. *CD-ROM Proceedings of the Nordic Workshop on Power and Industrial Electronics,* NORpie-02. Stockholm, Sweden. 1-5.
[18] Arshad, W. M., T. Bäckström, and C. Sadarangani. 2002. Evaluation of Different Electrical Machine Possibilities for an Integrated Free-piston Generator. CD-ROM *Proceedings of the 19th International Battery, Hybrid and Fuel-cell Electrical Vehicle Symposium (EVS-19).* Busan, Korea. 313-321.
[19] Aichlmayr, H. T. 2002. *Design Consideration Modeling, and Analysis of Micro-Homogeneous Charge Ignition Combustion Free-Piston Engine.* PhD Thesis Dissertation. University of Minnesota, USA.
[20] Brek, W. K., R. I. Stephens, and B. Dopker. 1993. Integrated Computational Durability Analysis. *ASME J. of Engineering for Industry.* 115(4): 492-497.
[21] Kuo, E. Y., and S. G. Kelkar. 1995. Vehicle Body Structure Durability Analysis. *SAE* Paper No. 951096.
[22] Kuo, E.Y., and S. G. Kelkar. 1995. Body Structure Durability Analysis. *Automotive Engineering.* 103(7): 73-77.
[23] Yim, H. J., and S. B. Lee. 1996. An Integrated CAE System for Dynamic Stress and Fatigue Life Prediction of Mechanical Systems. KSME *International Journal.* 10(2): 158-168.
[24] Liu, T.S. and E. J. Haug. 1986. *Computational Methods for Life Prediction of Mechanical Components of Dynamic Systems.* Technical Report 86-24, Centre for Computer Aided Design, University of Iowa, Iowa City, USA.
[25] Yim, H.J., and E. J. Haug. 1990. *Computational Methods for Dynamic Stress Analysis of Mechanical Systems.* PhD Thesis. College of Engineering, The University of Iowa, Iowa City, USA.
[26] Ryu, J., Sang S. Kim, and Sung S. Kim. 1992. An Efficient Computational Method for Dynamic Stress Analysis of Flexible Multibody Systems. *Computer and Structures.* 42(6): 969-977.
[27] Dowling, N.E. 1987. A Review of Fatigue Life Prediction Methods. SAE *Technical Paper,* Paper No. 871966.
[28] Dowling, N.E., 1999. *Mechanical Behaviour of Materials: Engineering Methods for Deformation, Fracture and Fatigue.* NJ, USA: Prentice Hall.
[29] Bannantine, S. A., J. J. Comer, and J. L. Handrock. 1990. *Fundamentals of Metal Fatigue Analysis.* New Jersey, USA: Prentice-Hall.
[30] Suresh, S. 2002. *Fatigue of Materials.* UK: Cambridge University Press.
[31] Stephens, R. I., A. Fatemi, R. R. Stephens, and H. O. Fuchs. 2001. Metal *Fatigue in Engineering.* USA: John Wiley and Sons, Inc.

[32] Kim, H. S., and C. B. Kim. 2002. Flexible Multibody Dynamic Analysis using Reduced Deformation Modes. *Proceedings of the First Asian Conference on Multibody Dynamics*. Iwaki, Japan, No. T313. 201-208.

[33] Wöhler, A. 1867. Wöhlers Experiment on the Strength of Metals. *Engineering*. 4: 160-161.

[34] Matsuishi M., and T. Endo T. 1968. Fatigue of Metals Subjected to Varying Stress. *Presented to JSME,* Fukuoko, Japan.

[35] Palmgren A. 1924. Durability of Ball Bearings. *ZVDI* 68(14): 339-341.

[36] Miner, M. A. 1945. Cumulative Damage in Fatigue. *Journal of Applied Mechanics*. 12: 159-164.

[37] Conle, F. A., and C. C. Chu. 1997. Fatigue Analysis and Vehicular *Structures*. *International Journal of Fatigue*. 19(1): S317-323.

[38] Savaidis, G. 2001. Analysis of Fatigue Behaviour of a Vehicle Axle Steering Arm based on Local Stresses and Strains. *Material Wwissenschaft und Werkstoff technik*. 32(4): 362-68.

[39] Juvinall, R. C., and K. M. Marshek. 1991. *Fundamentals of Machine Component Design*. New York : John Wiley and sons.

[40] Coffin L. F. Jr. 1964. A Study of the Effects of Cyclic Thermal Stresses on a Ductile Metal. *ASME Transactions*. 76: 931-950.

[41] Manson, S. S. 1953. Behaviour of Materials under Conditions of Thermal Stress. *Heat Transfer Symposium, University of Michigan Engineering Research Institute*, 9-75.

[42] Morrow, J. 1968. *Fatigue Design Handbook: Advances in Engineering*. Warendale, PA: SAE, 21-29.

[43] Smith, K. N., P. Watson, and T. H. Topper. 1970. A Stress-Strain Functions for the Fatigue on Materials. *Journal of Materials*. 5(4): 767-78.

[44] Wong, W. A. 1984. Monotonic and Cyclic Fatigue Properties of Automotive Aluminum Alloys. *SAE Technical Paper,* Paper No. 840120.

[45] Tucker, L., and S. Bussa. 1997. The SAE Cumulative Fatigue Damage Test Program: Fatigue under Complex Loading. *SAE Technical Paper* 3-14.

[46] Schaeffer, H. G. 2001. MSC.Nastran *Primer for Static Analysis*. USA: MSC.Software Corporation.

[47] Bishop, N. W. M., and F. Sherratt. 2000. *Finite Element Based Fatigue Calculations*. Kilbride, Glasgow: NAFEMS Ltd.